Conformation of PS–PMMA Diblock Copolymer in Toluene by Small Angle Neutron Scattering

C. C. Han* and B. Mozer

Institute for Materials Research, National Bureau of Standards, Washington, D.C. 20234.
Received July 23, 1976

ABSTRACT: A deuterated polystyrene–poly(methyl methacrylate) (dPS–PMMA) diblock copolymer and its deuterated polystyrene homopolymer precursor were studied by small angle neutron scattering and light scattering experiments using toluene as the solvent. The radii of gyration of the deuterated PS homopolymer (M = 88 000) measured by both methods and that of the PMMA block (M = 203 000) in the diblock copolymer measured only by neutron scattering were determined as 210 and 85 Å, respectively. In addition, the second virial coefficients and the chain excluded volume exponents were also obtained. The copolymer chain conformation in toluene at 23 °C is inferred from these measurements. It is suggested that the PMMA block forms the interior core from which the PS block exudes out as an expanded chain.

I. Introduction

Block copolymers have been studied extensively for the past decade.[1] However, there is a controversy with regard to the chain conformation of the block copolymer with noncompatible blocks in dilute solution.[2-8] The crux of the issue is whether or not the block copolymer assumes a "segregated" or a "nonsegregated" conformation; do the noncompatible blocks A and B segregate into different domains because of the large repulsive interactions between them, or do they assume a uniformly interpenetrating conformation with a large number of contact points between unlike segments that gives rise to chain expansion beyond that expected in their respective homopolymer states?

Attempts to elucidate this problem have been made.[7-10] A diblock copolymer (A–B) was dissolved in a solvent which is isorefractive with one (B) of the two blocks (A–B) and a light scattering study made on the chain conformation of the other block (A). In conjunction with the conformational characterization of the same block (A) in the same solvent in the homopolymer state, one could, in principle, deduce the conformation of the A–B block copolymer. Unfortunately anomalous upward curvatures of the Zimm plot were observed instead of the regular straight line grid. Although various theories[7-9] have been proposed to explain this "anomaly", the central question of the block copolymer conformation has been elusive and further enshrouded by competing models used to explicate the said anomaly.

We therefore attacked the problem with an additional experimental tool, the small angle neutron scattering (SANS). Our approach was simply to probe with neutrons the first block (B) inaccessible to study by visible light then to probe with visible light the second block (A) which was undetectable using neutrons. With additional light scattering study of the second block (A) in the homopolymer state; we were able to draw a more complete picture of a diblock copolymer conformation in a given solvent. We used an anionically polymerized deuterated polystyrene–poly(methyl methacrylate) (dPS–PMMA) diblock copolymer in deuterated toluene for the SANS experiment and in protonated toluene for the light scattering experiment. Owing to the large difference in the contrast factor for PMMA and dPS (see below), we sample only the PMMA block in deuterated toluene by the SANS technique. Correspondingly, because of the large difference in the differential refractive index increments for the two blocks in toluene (PMMA is isorefractive with toluene), we measure only the dPS block by the light scattering technique. It should be noted that the chemical nature of the solvent is essentially the same for both kinds of measurements.

In the following section we will first examine the theory of small angle neutron scattering and its relationship with light scattering. Next, we outline the experimental details of the two kinds of scattering experiments and of the sample preparation. Finally, we discuss the results of the analysis of the scattering experiments and the conformation characterization of dPS–PMMA diblock copolymer in toluene.

II. Theory of Small Angle Neutron Scattering

Small angle neutron scattering has recently been used in the study of polymer systems in bulk as well as in solution.[11-17] This technique has shown great promise in polymer research for the following two reasons: (1) the large accessible range of scattering wave vector q (or momentum transfer vector, with $q = |\mathbf{q}|$), where q^{-1} easily covers the range between a few ångströms to several hundred ångströms; (2) the large difference of scattering length for different isotopes, especially between protons and deuterons. This allows selective study of some labeled molecules in a scattering system or some labeled parts of a polymer molecule. We shall discuss this selective study subsequently.

We wish to examine the theory of neutron scattering from polymers in solution in the limit where the momentum transfer approaches zero. The neutron scattering will then be probing distances in the system much longer than the distance between solvent molecules or between monomer units of a polymer molecule. In the static limit the coherent scattering cross section is[18]

$$\frac{\partial\sigma}{\partial\Omega} = \left\langle \left| \sum_{i,\alpha} b_{i\alpha} e^{-i\mathbf{q}\cdot(\mathbf{r}_i+\mathbf{x}_{i\alpha})} \right|^2 \right\rangle = \left\langle \sum_{i,\alpha}\sum_{j,\beta} b_{i\alpha} b_{j\beta} e^{-i\mathbf{q}\cdot(\mathbf{r}_i+\mathbf{x}_{i\alpha}-\mathbf{r}_j-\mathbf{x}_{j\beta})} \right\rangle \quad (1)$$

where $\mathbf{q} = \mathbf{k}_f - \mathbf{k}_0$ is the vector difference between the incoming neutron wave vector $\mathbf{k}_0$ and the scattered neutron wave vector $\mathbf{k}_f$, with $|q| = 4\pi/\lambda \sin\theta/2$, λ is the incoming neutron wavelength and θ is the scattering angle, $b_{i\alpha}$ is the scattering length, and $x_{i\alpha} = |\mathbf{x}_{i\alpha}|$ is the distance from the center of the mass of the ith scattering element at $\mathbf{r}_i$ to the αth nucleus. The angular bracket $\langle\ \rangle$ refers to an ensemble average for the whole system.

Here, we have defined a scattering element i as a volume element with a dimension (~10 Å) longer than the intermolecular distances of solvent molecules, and also longer than the thickness of the solvent molecule layer which is surrounding the polymer segment. This solvent molecule layer structure may differ from the pure solvent structure because of the polymer–solvent interaction. The dimension of this scattering element is still much smaller than the dimension of a whole polymer molecule. In other words, a scattering el-

ement of a polymer means a volume element centered at the center of mass of a polymer segment which includes this polymer segment of one or several monomer units and its surrounding solvent molecule layer. Similarly, a scattering element for the solvent means a volume element of the same size as defined for a polymer element but which includes only a few solvent molecules. The structure of the solvent scattering element is assumed identical with that in pure solvent. We shall define an average scattering length for a solvent or polymer scattering element as

$$\bar{a}_i(\mathbf{q}) \equiv \sum_{\alpha} b_{i\alpha} e^{-i\mathbf{q}\cdot\mathbf{x}_{i\alpha}} \tag{2}$$

where the sum goes over all nuclei in all the atoms in this scattering element. For the condition $|\mathbf{q}\cdot\mathbf{x}_{i\alpha}| \ll 1$, $a_i(\mathbf{q})$ is essentially a constant and given by

$$\bar{a}_i(\mathbf{q}) \cong \sum_{\alpha} b_{i\alpha} = \bar{a}_i \tag{3}$$

Substituting eq 3 into eq 1, we find the total scattering cross section or scattering intensity, $i(\mathbf{q})$, including incoherent scattering[18] for a polymer solution, is given by

$$\begin{aligned} i(\mathbf{q}) &= \left\langle \left| \sum_{i}^{n_m} \bar{a}_i e^{-i\mathbf{q}\cdot\mathbf{r}_i} + \sum_{k}^{n_s} \bar{a}_k e^{-i\mathbf{q}\cdot\mathbf{r}_k} \right|^2 \right\rangle + I_s \\ &= \left\langle \sum_{i,j}^{n_m} \bar{a}_i \bar{a}_j e^{-i\mathbf{q}\cdot(\mathbf{r}_i - \mathbf{r}_j)} \right\rangle \\ &\quad + 2 \left\langle \sum_{i}^{n_m} \sum_{k}^{n_s} \bar{a}_i \bar{a}_k e^{-i\mathbf{q}\cdot(\mathbf{r}_i - \mathbf{r}_k)} \right\rangle \\ &\quad + \left\langle \sum_{k,l}^{n_s} \bar{a}_k \bar{a}_l e^{-i\mathbf{q}\cdot(\mathbf{r}_k - \mathbf{r}_l)} \right\rangle + I_s \\ &= i_{mm}(\mathbf{q}) + i_{ms}(\mathbf{q}) + i_{ss}(\mathbf{q}) + I_s \end{aligned} \tag{4}$$

where the n_m and n_s are total number of polymer and solvent scattering elements in the whole scattering system. I_s is the sum of any spin incoherence and isotopic incoherence that might occur in the system.

First, let us examine the $i_{ss}(\mathbf{q})$ term, which is the scattering only from the correlation between one solvent element and another solvent element. These solvent elements can be viewed as a set of pure solvent elements having some holes mixed in. The probability of finding a solvent element k at $\mathbf{r}_k$ with a solvent element l at $\mathbf{r}_l$ can be represented by P_{ss}. The deviation of P_{ss} from unity can be caused by fluctuations (neglect the short-range structure) such as thermal fluctuation. Also we would like to use the probability function P_{sH}, defined by Hyman,[19] which is one if kth and lth elements are both solvent elements and zero if either kth or lth is a polymer element. The term $i_{ss}(q)$ can then be written as follows with $\bar{a}_s$ as the scattering length of a solvent scattering element

$$\begin{aligned} i_{ss}(\mathbf{q}) = \bar{a}_s{}^2 \sum_{k,l}^{n=n_m+n_s} &[(P_{ss} - 1)P_{sH} e^{-i\mathbf{q}\cdot(\mathbf{r}_k - \mathbf{r}_l)} \\ &+ P_{sH} e^{-i\mathbf{q}\cdot(\mathbf{r}_k - \mathbf{r}_l)}] \end{aligned} \tag{5}$$

Following Hyman's approach, if we neglect the effect due to a small number of solvent elements near the holes which have contributions to the $i_{ss}(\mathbf{q})$ slightly different from pure solvent in the case $n_m \ll n_s$

$$\begin{aligned} i_{ss}(\mathbf{q}) &\cong \bar{a}_s{}^2 \sum_{k,l}^{n_s} (P_{ss} - 1) e^{-i\mathbf{q}\cdot(\mathbf{r}_k - \mathbf{r}_l)} + \bar{a}_s{}^2 \sum_{k,l}^{n} P_{sH} e^{-i\mathbf{q}\cdot(\mathbf{r}_k - \mathbf{r}_l)} \\ &= \bar{a}_s{}^2 \sum_{k,l}^{n_s} (P_{ss} - 1) e^{-i\mathbf{q}\cdot(\mathbf{r}_k - \mathbf{r}_l)} \\ &\quad + \bar{a}_s{}^2 \left\langle \sum_{k,l}^{n_s} e^{-i\mathbf{q}\cdot(\mathbf{r}_k - \mathbf{r}_l)} \right\rangle_{n_m} \end{aligned} \tag{6}$$

where $\langle\ \rangle_{n_m}$ means ensemble average over all the possible polymer elements (or hole) configurations.

This means that the scattering due to the solvent elements in the polymer solution can be approximated by two contributions. The first term above represents the structure of the solvent which is similar to that of pure solvent. The second term represents the scattering due to the presence of holes in a otherwise uniform solvent medium. The structure part has been separated out into the first term. Let $i_{ss}{}^0(\mathbf{q})$ be the scattering for pure solvent and $n_s{}^0 = n = n_m + n_s$ then

$$i_{ss}{}^0(\mathbf{q}) = \bar{a}_s{}^2 \sum_{k,l}^{n_s{}^0} (P_{ss} - 1) e^{-i\mathbf{q}\cdot(\mathbf{r}_k - \mathbf{r}_l)} + I_s{}^0$$

and

$$i_{ss}(\mathbf{q}) + I_s - \frac{n_s}{n_s{}^0} i_{ss}{}^0(\mathbf{q}) = \bar{a}_s{}^2 \left\langle \sum_{k,l}^{n_s} e^{-i\mathbf{q}\cdot(\mathbf{r}_k - \mathbf{r}_l)} \right\rangle + I_s'' \tag{7}$$

where I_s is the sum of the incoherent scattering caused by solvent (I_s') and polymer (I_s''), I_s' can be eliminated through solvent subtraction because $I_s' = (n_s/n_s{}^0) I_s{}^0$ and I_s'' can also be eliminated through the subtraction of incoherent scattering caused by the same number of monomers as in the polymers. We will further discuss this in the experimental section.

Considering the cross term $i_{ms}(\mathbf{q})$, we shall call P_{ms} the probability function of finding a solvent element j at $\mathbf{r}_j$ given a polymer element i at $\mathbf{r}_i$. Since we have restricted ourselves to long range correlations only the solvent element at r_j does not know whether the ith element is a polymer or a solvent element. Therefore, P_{ms} should be similar to P_{ss}, and we can write $i_{ms}(\mathbf{q})$ as follows

$$\begin{aligned} i_{ms}(\mathbf{q}) &= 2\bar{a}_m \bar{a}_s \left\langle \sum_{i}^{n_m} e^{-i\mathbf{q}\cdot\mathbf{r}_i} \cdot \sum_{j}^{n_s} P_{ss} e^{i\mathbf{q}\cdot\mathbf{r}_j} \right\rangle_{n_m} \\ &= 2\bar{a}_m \bar{a}_s \left[\left\langle \sum_{i}^{n_m} e^{-i\mathbf{q}\cdot\mathbf{r}_i} \cdot \sum_{j}^{n_s} e^{i\mathbf{q}\cdot\mathbf{r}_j} \right\rangle_{n_m} \right. \\ &\quad \left. + \left\langle \sum_{i}^{n_m} e^{-i\mathbf{q}\cdot\mathbf{r}_i} \cdot \sum_{j}^{n_s} (P_{ss} - 1) e^{i\mathbf{q}\cdot\mathbf{r}_j} \right\rangle_{n_m} \right] \end{aligned} \tag{8}$$

with $\bar{a}_m$ as the scattering length of a polymer scattering element. Using the property of a uniform medium and neglecting the edge effect of the total scattering volume, then

$$\left\langle \sum_{i}^{n} e^{-i\mathbf{q}\cdot\mathbf{r}_i} \right\rangle = \sum_{i}^{n} e^{-i\mathbf{q}\cdot\mathbf{r}_i} = 0$$

and

$$\sum_{i}^{n_s} e^{-i\mathbf{q}\cdot\mathbf{r}_i} = -\sum_{i}^{n_m} e^{-i\mathbf{q}\cdot\mathbf{r}_i} \tag{9}$$

We can compare the relative contribution of the two terms in eq 8. Assume solvent element and polymer element are uncorrelated, we could obtain the ratio R of these two terms as follows

$$\begin{aligned} R &= -\frac{\left\langle \sum_{i}^{n_m} e^{-i\mathbf{q}\cdot\mathbf{r}_i} \right\rangle_{n_m} \left[\sum_{j}^{n_s} (P_{ss} - 1) e^{i\mathbf{q}\cdot\mathbf{r}_j} \right]}{\left\langle \sum_{i}^{n_m} \sum_{j}^{n_m} e^{-i\mathbf{q}\cdot(\mathbf{r}_i - \mathbf{r}_j)} \right\rangle_{n_m}} \\ &= -\frac{\left\langle \sum_{i}^{n_m} e^{-i\mathbf{q}\cdot\mathbf{r}_i} \right\rangle_{n_m} \left[\sum_{j}^{n_s} (P_{ss} - 1) e^{i\mathbf{q}\cdot\mathbf{r}_j} \right]}{n_m \left\langle \sum_{k}^{n_m} e^{-i\mathbf{q}\cdot\mathbf{r}_k} \right\rangle_{n_m}} \end{aligned}$$

or

$$|R| \cong \frac{1}{n_m} \ll 1$$

Therefore

$$i_{ms}(\mathbf{q}) \cong -2\bar{a}_m\bar{a}_s \left\langle \sum_{i,j}^{n_m} e^{-i\mathbf{q}\cdot(\mathbf{r}_i-\mathbf{r}_j)} \right\rangle_{n_m}$$

and since

$$i_{mm}(\mathbf{q}) = \bar{a}_m{}^2 \left\langle \sum_{i,j}^{n_m} e^{-i\mathbf{q}\cdot(\mathbf{r}_i-\mathbf{r}\cdot j)} \right\rangle_{n_m}$$

therefore

$$I(\mathbf{q}) \equiv i(\mathbf{q}) - \frac{n_s}{n_s{}^0} i_{ss}{}^0(\mathbf{q}) - I_s''$$

$$= (\bar{a}_m{}^2 - 2\bar{a}_m\bar{a}_s + \bar{a}_s{}^2) \left\langle \sum_{i,j}^{n_m} e^{-i\mathbf{q}\cdot(\mathbf{r}_i-\mathbf{r}_j)} \right\rangle_{n_m}$$

$$= (\bar{a}_m - \bar{a}_s)^2 \left\langle \sum_{i,j}^{n_m} e^{-i\mathbf{q}\cdot(\mathbf{r}_i-\mathbf{r}_j)} \right\rangle \quad (10)$$

here we have dropped the n_m from eq 10 for convenience. This scattering intensity $I(\mathbf{q})$ which is due to the presence of polymer molecules in the solution may now be rewritten in terms of the center of mass coordinates of individual polymer molecules (the solvent molecules associated with polymer elements will have to be considered as part of the polymer) as

$$I(\mathbf{q}) = (\bar{a}_m - \bar{a}_s)^2 \left\langle \left(\sum_{j}^{N} \sum_{m}^{\sigma} e^{-i\mathbf{q}\cdot(\mathbf{R}_j+\mathbf{r}_{jm})} \right) \times \left(\sum_{k}^{N} \sum_{l}^{\sigma} e^{i\mathbf{q}\cdot(\mathbf{R}_k+\mathbf{r}_{kl})} \right) \right\rangle$$

$$= (\bar{a}_m - \bar{a}_s)^2 \left\langle \sum_{j=k}^{N} \left(\sum_{m,l}^{\sigma} e^{-i\mathbf{q}\cdot(\mathbf{r}_{jm}-\mathbf{r}_{jl})} \right) + \sum_{j\neq k}^{N} \left(\sum_{m}^{\sigma} e^{-i\mathbf{q}\cdot\mathbf{r}_{jm}} \cdot \sum_{l}^{\sigma} e^{i\mathbf{q}\cdot\mathbf{r}_{kl}} \right) e^{-i\mathbf{q}\cdot(\mathbf{R}_j-\mathbf{R}_k)} \right\rangle \quad (11)$$

where N is the number of polymer molecules, σ is the number of elements per polymer molecule, $\mathbf{R}_j$ is the position of the center of mass of the jth polymer molecule, and $\mathbf{r}_{jm}$ is the position of the mth element of the jth polymer from its center of mass. Two important points about eq 11 should be noted: (1) eq 11 is essentially the same expression as for light scattering or small angle x-ray scattering theory for polymer solutions with the only difference being the excess scattering cross section or the contrast factor $(\bar{a}_m - \bar{a}_s)^2$, and (2) for the block copolymer case, eq 10 should be written as

$$I(\mathbf{q}) = \left\langle \left| (\bar{a}_m - \bar{a}_s) \sum_{i}^{n_m} e^{-i\mathbf{q}\cdot\mathbf{r}_i} + (\bar{a}_m{}' - \bar{a}_s) \sum_{j}^{n_m{}'} e^{-i\mathbf{q}\cdot\mathbf{r}_j} \right|^2 \right\rangle \quad (12)$$

where $\bar{a}_m$, $\bar{a}_m{}'$, r_i, and r_j are the average coherent scattering lengths and positions of the A and B type of polymer segments. The corresponding light scattering theory for the block copolymers has been developed over the years,[20] and it requires no discussion here. For the SANS when $|\bar{a}_m - \bar{a}_s| \gg |\bar{a}_m{}' - \bar{a}_s|$, eq 12 reduces to eq 11.

Following the derivation by Zernicke and Prins[21] or Debye and Menke,[22] eq 11 can now be expressed as:

$$I(\mathbf{q}) = (\bar{a}_m - \bar{a}_s)^2 \times \left[N\langle F(\mathbf{q})^2\rangle + \langle F(\mathbf{q})\rangle^2 \left\langle \sum_{j\neq k}^{N} e^{-i\mathbf{q}\cdot(\mathbf{R}_j-\mathbf{R}_k)} \right\rangle \right]$$

$$= (\bar{a}_m - \bar{a}_s)^2 \left[N\langle F(\mathbf{q})^2\rangle + \langle F(\mathbf{q})\rangle^2 \frac{N^2}{V} \times \int_V P(\mathbf{R}_{ij}) e^{-i\mathbf{q}\cdot R_{ij}}\, dV \right] = (\bar{a}_m - \bar{a}_s)^2 N\langle F(\mathbf{q})^2\rangle \times \left[1 + \frac{N}{V} \left(\int_V (g(\mathbf{r}) - 1) e^{-i\mathbf{q}\cdot\mathbf{r}}\, d\mathbf{r} \right) \right] \quad (13)$$

where

$$\langle F(\mathbf{q})\rangle \equiv \left\langle \sum_{m}^{\sigma} e^{-i\mathbf{q}\cdot\mathbf{r}_{jm}} \right\rangle$$

$g(\mathbf{r})$ is the pair correlation function for the center of mass of polymer molecules, $P(\mathbf{R}_{ij})$ is the probability of finding a polymer molecule j at position $\mathbf{R}_j$, when polymer molecule i is located at position $\mathbf{R}_i$, and $\langle F(\mathbf{q})^2\rangle = \langle F(\mathbf{q})\rangle^2$ under the assumption of spherical symmetry for the segment distribution within a given polymer molecule. Equation 13 can also be expressed as

$$I(\mathbf{q}) = (\bar{a}_m - \bar{a}_s)^2 N \left\langle \sum_{i,j}^{\sigma} e^{-i\mathbf{q}\cdot\mathbf{r}_{ij}} \right\rangle \left[1 + \frac{N}{V} \int h(\mathbf{r}) e^{-i\mathbf{q}\cdot\mathbf{r}}\, d\mathbf{r} \right]$$

$$= (\bar{a}_m - \bar{a}_s)^2 N\sigma^2 P(\mathbf{q}) \left[1 + \frac{N}{V} \int h(\mathbf{r}) e^{-i\mathbf{q}\cdot\mathbf{r}}\, d\mathbf{r} \right]$$

$$= (\bar{a}_m - \bar{a}_s)^2 N\sigma^2 P(\mathbf{q}) S'(\mathbf{q}) \quad (14)$$

where $P(\mathbf{q}) = (1/\sigma^2)\langle \Sigma_{i,j}{}^{\sigma} e^{-i\mathbf{q}\cdot\mathbf{r}_{ij}}\rangle$ is the particle scattering function for the single polymer molecule and the total correlation function $h(\mathbf{r})$ for polymer molecules is defined as

$$h(\mathbf{r}) \equiv g(\mathbf{r}) - 1$$

The total structure factor is proportional to the product of the internal structure factor $P(\mathbf{q})$ and the external structure factor in the bracket [ ].

The total structure factor or intensity reduces to the internal part $P(\mathbf{q})$ as concentration approaches zero. As is usual in light scattering theory, $P(\mathbf{q})$ can be expanded in terms of even moments of the segment pair distribution. In the limit of small $\mathbf{q}$, $P(\mathbf{q})$ reduces to[23]

$$P(\mathbf{q}) = \frac{1}{\sigma^2} \sum_{i,j}^{\sigma} \left(1 - \frac{q^2\langle \mathbf{r}_{ij}{}^2\rangle}{3!} + \dots \right) = 1 - \frac{q^2\langle R_G{}^2\rangle}{3} + \dots \quad (15)$$

As both concentration c and q approach zero, the ratio c/I becomes

$$\lim_{\substack{c\to 0 \\ q\to 0}} \frac{c}{I} = A \left(1 + \frac{q^2\langle R_G{}^2\rangle}{3} \right) \quad (16)$$

The particle scattering functions $P(\mathbf{q})$ for various types of particle shapes and polymer segmental distribution functions are all well known.[20] In order to take into account the effect of long-range perturbation of volume exclusion for random coil polymer, an excluded volume exponent ν has been proposed[24-27] as a measure of chain expansion. Those authors suggest that if $\langle r_{ij}{}^2\rangle \propto |i-j|^{\nu}$ then

$$\lim_{x\to\infty} P(\mathbf{q}) = Ax^{-1/\nu} \quad (17)$$

where $x = q^2\langle R_G{}^2\rangle$. Contrary to light scattering experiment, the asymptotic limit of large x is readily achieved in the SANS and ν can be obtained directly from the slope of ln $P(\mathbf{q})$ vs. ln q^2 plot.

III. Experimental Section

(1) Small Angle Neutron Scattering. The small angle neutron scattering (SANS) experiments were performed at the NBS research reactor. The experimental facility as shown in Figure 1 consists of equipment to provide a long wavelength beam of neutrons, a diffractometer to measure the scattered neutron beam as a function of the scattering angle, and a sample cell and temperature controller to hold the samples at fixed position and temperature during the course of the experiments.

A collimated long wavelength beam of neutrons is extracted from the reactor after transmission through a 7.62 cm quartz filter, F_1, and a crude Soller slit horizontal collimator, C_1, of 42′ of arc. The beam

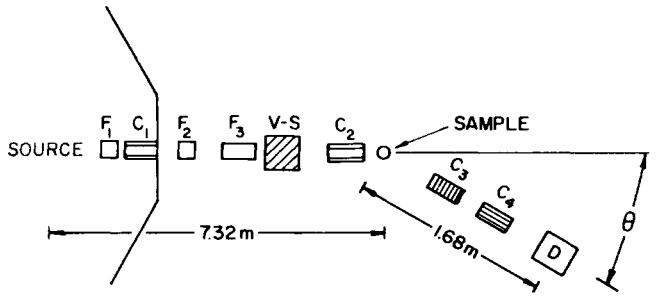

Figure 1. A block diagram of the small angle neutron scattering spectrometer. Here, F_1, F_2, F_3 are filters; C_1, C_2, C_3, C_4 are Soller slit collimators; VS is a helical velocity selector.

then is transmitted through 5.08 cm of a warm beryllium filter, F_2, to remove more fast neutrons before it is partially monochromated by a refrigerated 25.48 cm beryllium filter, F_3. A helical velocity selector, VS, with a fixed wavelength spread of 1.0 Å further monochromates the beam; a 5 Å beam of neutrons was used for these experiments. The horizontal divergence of the neutron beam impinging on the sample is further defined by a Soller slit collimator, C_2, of 10′ of arc. The vertical divergence of the impinging beam is defined by the distance of sample from the neutron source in the reactor and the size of that source and the sample. The vertical divergence of the beam for these experiments was 15′ of arc. A beam monitor for normalization of the data was attached to the exit end of collimator C_2.

The sample cell was constructed of a thin walled aluminum alloy cylinder of diameter 1 cm and height 4.5 cm. The sample cell was attached to a large copper block which was maintained at constant temperature, 23 ± 0.5 °C. Cadmium plates were inserted in the top and bottom of the sample cell to prevent scattering from the thicker parts of the sample cell and copper block. The sample cell and copper block were mounted in a thin walled aluminum thermal shield which was centered at the pivot point of the diffractometer.

The scattered neutrons were measured by a detector on the movable arm of a diffractometer after passing through a 10′ Soller slit horizontal collimator, C_3, and a Soller slit vertical collimator, C_4, which can be varied from a minimum of 20′ of arc. For these experiments no Soller slits were used in the vertical collimator and the vertical divergence of the scattering beam was determined by the acceptance angle of the detector which was 80′ of arc. Scattering data on this instrument were taken only over an angular range from 0.5 to 8.5° scattering angle. The data were taken automatically using the computer control system at the NBS reactor. Complete sweeps of the angular scan were taken and repeated until a desired statistical accuracy was achieved. This procedure allowed a close control of any errors that might arise from drifts in the electronics or angular errors in the scan. Angular measurements were very reproducible and any error in a given scattering angle was about 1′ of arc. The zero angle was initially determined by a precise optical alignment then checked by a scan of the impinging beam whose intensity was reduced by a thin cadmium absorber. The final zero determination was made by comparing the scattering for equivalent positive and negative angles. Our error in the zero angle is at most 2′ of arc.

Scattering data on the SANS instrument were taken on the empty aluminum sample cell, deuterated toluene, and various concentrations of the polymers in the deuterated toluene, and mixtures of toluene-*d* with corresponding fractions of monomers contained in solutions. We considered toluene our standard for the experiment and repeated many scattering scans of it to ensure ourselves that the instrument and electronics were stable over the period of time necessary to obtain a high statistical accuracy for each solution. This allowed us to calculate the difference in the scattering between the polymers in solution and the solvent and reliably assign errors as arising solely from the statistical accuracies of the scattering scans. Data points in the extreme forward direction were not that reliable because of the proximity of the forward beam of neutrons which could produce errors greater than statistical for slight errors arising from the mechanical positioning of the diffractometer.

(2) Light Scattering. A SOFICA[41] light scattering photometer with vertically polarized incident light at λ 5461 Å was used for the light scattering experiment. The measurement was carried out at 23 °C and with a vertical analyzer. Pure benzene was used as the standard with the Rayleigh ratio for vertical polarization in green light of 17.82×10^{-6} cm^{-1} which is calculated from the literature value[28] of 15.8×10^{-6} cm^{-1} for the unpolarized case and depolarization ratio of 0.41. Scattering intensities were measured over the range of 30 to 150° for all the solutions and solvent used. The refractive index increments, dn/dc, were obtained from the literature[29] as tabulated in Table I.

Table I
Constants Used for the LS and the SANS Measurements

Solvent	n	dn/dc, ml/g	
		PS	PMMA
Toluene	1.495	0.1073	0.003

Atom	Coherent scattering length $b \times 10^{12}$, cm
H	−0.374
D	0.667
C	0.665
O	0.577

Element	Av coherent scattering length $\bar{a} \times 10^{12}$, cm
Toluene-*d* (C_7D_8)	9.99
Styrene-*d* (C_8D_8)	10.66
Methyl methacrylate ($C_5H_8O_2$)	1.49

(3) Sample Preparation. A deuterated polystyrene–poly(methyl methacrylate) diblock copolymer was kindly prepared for us by Professor H. Yu at the University of Wisconsin. Deuterated styrene and methyl methacrylate were purified with sodium dispersion and distilled under vacuum. The anionic polymerization[30] was carried out with *sec*-butyllithium as the initiator and tetrahydrofuran as solvent. The crossover reagent from the styrylolithium growing end to the methyl methacrylate lithium complex was 1,1-diphenylethylene. A part of the "living" dPS precursor was terminated for later analysis. Extraction with boiling cyclohexane was effected to remove any remaining homopolymer of dPS in the final diblock copolymer. The weight fraction of dPS (W_{dPS}) in the block copolymer was measured by elementary analysis as 0.303. Clarification of solutions used in light scattering was effected by filtration under ambient pressure through 0.22 μm Millipore filter.

IV. Results and Discussion

Before presenting the results of the SANS, a brief discussion of the contrast factor for the different blocks, excess scattering intensity, and average wavelength is in order.

The coherent scattering lengths of four kinds of atoms involved in the block copolymer and solvent are collected in Table I.[31] The monomer unit and solvent molecule may have slightly different molecular volume, the volume correction to the mean coherent length is effected by use of the simple linear relationship

$$\bar{a}_m' = \bar{a}_m \cdot \frac{v_s}{v_m} = \bar{a}_m \frac{M_s \rho_m}{\rho_s M_m} \tag{18}$$

where the ρ_m and ρ_s are densities of the polymer and the solvent, and M_m and M_s are the molecular weights of a monomer unit and a solvent molecule. The packing density difference of solvent molecules in a polymer element and in a solvent element are neglected, and with the densities of *d*-toluene, dPS, and PMMA as 0.95, 1.13, and 1.19 ml/g, respectively, we obtain the contrast ratio of PMMA to dPS in toluene

$$\frac{\bar{a}_{PMMA}' - \bar{a}_{d\text{-tol}}}{\bar{a}_{dPS}' - \bar{a}_{d\text{-tol}}} \cong 7$$

If we also include the ratio of the degree of polymerization, the ratio of the scattering intensity from the PMMA block to that of the dPS block is about 20.

We can safely assume that the effect of neglecting the contribution from dPS of our block copolymer in toluene-*d* to the total intensity is insignificant.

The excess scattering intensity I_e at any angle owing to the

presence of polymer molecules in the solution is actually obtained from the difference of the solution scattering intensity, I_s, and what we call the background scattering intensity, I_b, as shown in eq 19 below. I_b is the total scattering intensity of a mixture of solvent and monomers which has a concentration equivalent to that of the solution (in terms of monomer atom percent). The scattering intensities of solution and background are again the differences between the actual measured intensities I_s', I_b' and that part from the aluminum cell including a transmission (T_s, T_b) correction.

$$I_e = I_s - I_b = (I_s' - I_{cell} \times T_s) - (I_b' - I_{cell} \times T_b) \quad (19)$$

This subtraction procedure allows us to best determine that part of the coherent scattering arising solely from the polymer in solution because the monomer–solvent mixture will produce the same incoherent scattering and approximately the same multiple scattering as the polymer solution.

Collimation corrections were done on I_e through an algebraic matrix inversion method[32] yielding I_c. The corrected intensity $I_c(\mathbf{q})$ should then be proportional to $I(\mathbf{q})$ in eq 11 through eq 16.

The average wavelength used for the radius of gyration measurement must be the inverse square average according to eq 15

$$\bar{\lambda}^{-2} = \int \frac{1}{\lambda^2} i(\lambda)\, d\lambda / \int i(\lambda)\, d\lambda$$

and in this experiment $\bar{\lambda}$ is 4.78 Å.

In Figure 2, we present the raw data of our SANS measurements for three systems, toluene-*d*, 1% solution of dPS in toluene-*d* and 2% solution of dPS–PMMA in toluene-*d*. The results of SANS data after subtracting the background contribution in conjunction with collimation corrections are shown in Figure 3.

In Figure 4, the Zimm plot of the diblock copolymer in toluene-*d* from the SANS data is shown. The radius of gyration of the PMMA block thus obtained was 85 ± 7 Å. One should note the lack of a concentration dependence of the scattering intensity along the extrapolated $\theta = 0$ line which indicates that the second virial coefficient A_2 would be zero if this were a homopolymer case. Since this is a block copolymer system, the zero concentration dependence could have a quite different meaning and we shall discuss this later. In Figure 5, we show the Zimm plot of this diblock copolymer in toluene from LS. Since PMMA is isorefractive with toluene, what we measure in LS is the dPS block in contrast to the previous SANS case. The radius of gyration for the dPS block in toluene was determined as 225 ± 40 Å. The molecular weight of the dPS block from the intercept of Figure 5 (after weight fraction correction) was determined to be (95 ± 3) × 10^3.

Returning to the SANS and LS measurements of the dPS precursor in toluene-*d* and toluene, respectively, we show the Zimm plot of the SANS results in Figure 6. Though the excess scattering of dPS homopolymer in *d*-toluene was small, we were still able to extract the conformation parameter and found it to be consistent with that deduced from the light scattering. The radius of gyration obtained through eq 16 was 210 ± 40 Å which is to be compared with 215 ± 18 Å from the LS measurement. The molecular weight of the precursor was found as (88 ± 3) × 10^3 from the LS which is consistent with (95 ± 3) × 10^3 for the dPS block in the copolymer. A summary of all the measurements is collected in Table II.

It seems clear from the foregoing that our approach to the problem has indeed provided us with a consistent set of data, not only for cross comparison of the block copolymer with both scattering techniques, but also for a comparison of the precursor and its counterpart in the copolymer with a given

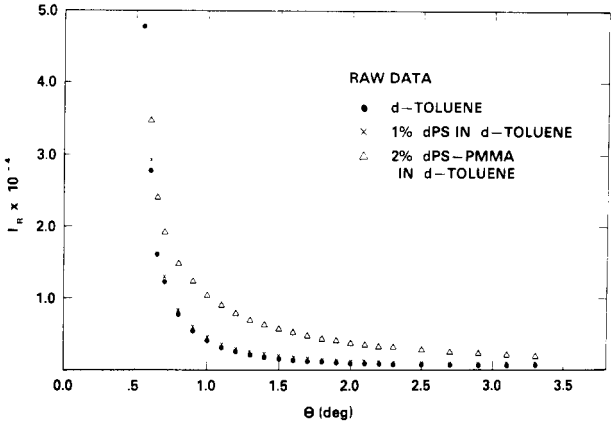

Figure 2. Typical raw data from neutron scattering of tolune-*d* (●), 1% dPS in tolune-*d* (×), and 2% dPS–PMMA in toluene-*d* (△).

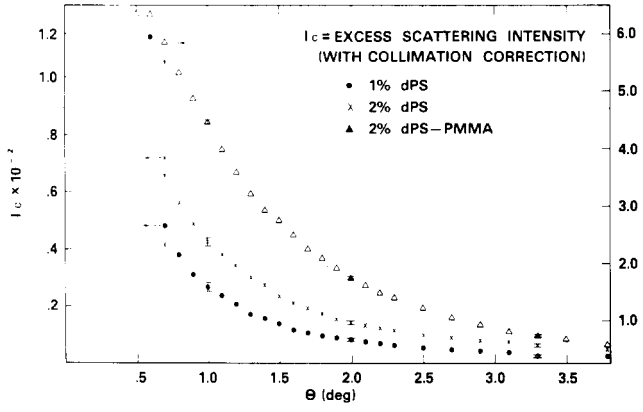

Figure 3. Excess intensity from neutron scattering of 1% dPS (●), 2% dPS (×), and 2% dPS–PMMA (△) all in toluene-*d*.

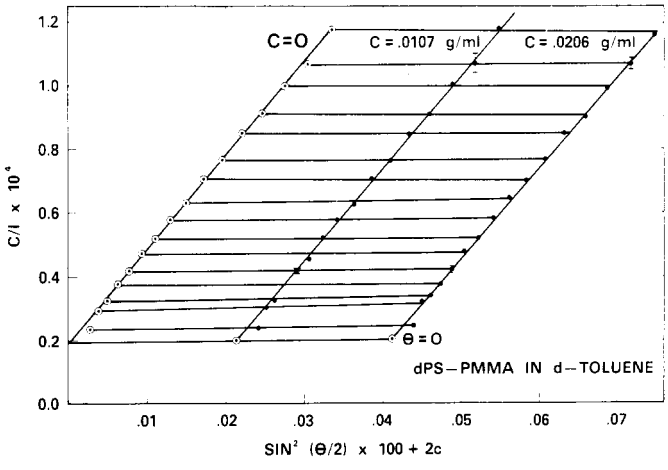

Figure 4. Zimm plot from neutron scattering data of dPS–PMMA in toluene-*d*.

technique, i.e., light scattering. These results may be summarized as shown below

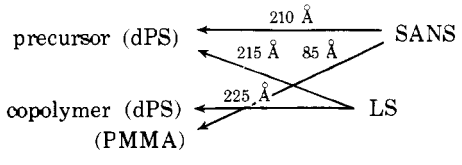

By virtue of the small wavelength (5 Å) of the incident neutron, the SANS technique furnishes an additional con-

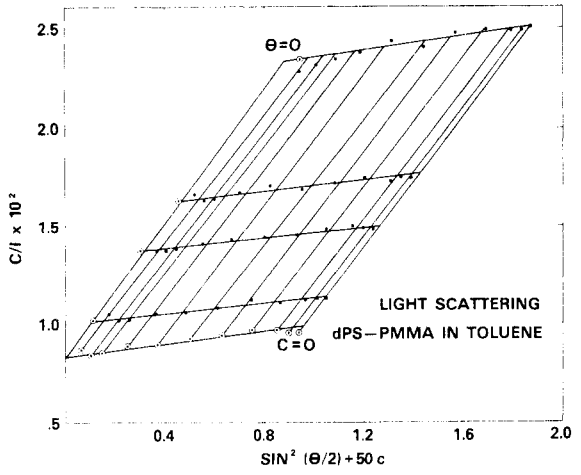

Figure 5. Zimm plot from light scattering data of dPS–PMMA in toluene-*d*.

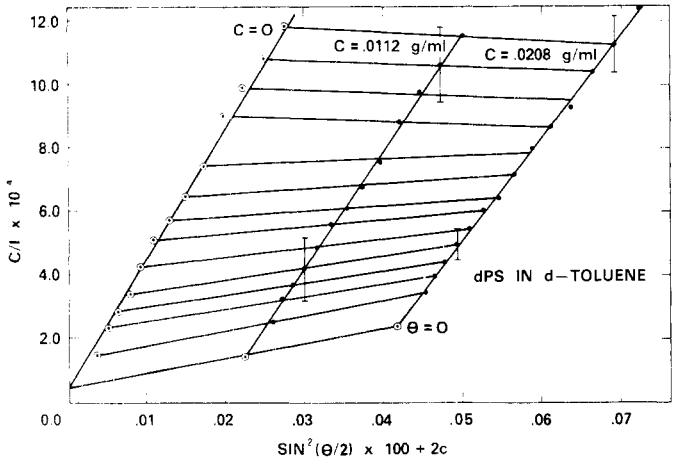

Figure 6. Zimm plot from neutron scattering data of dPS in toluene-*d*.

figurational parameter, namely the excluded volume exponent defined in eq 17. The data up to the large scattering angle limit are graphically presented in Figure 7. The excluded volume exponent for the PMMA block as obtained from the ln I_c vs. ln $\sin^2(\theta/2)$ plot is 1.04 ± 0.06 and 1.03 ± 0.05 for the two different concentrations. This is essentially unity within our uncertainty limit. Also in the plot we can see that the data deviate from a straight line as we go to larger q. This deviation as $q \gtrsim 0.1$ Å^{-1} probably comes from the syndiostructure of PMMA which has been discussed by Yoon and Flory.[33] For a matter of comparison, the ν for a commercially available homo-PMMA homopolymer (with M_w = 60 600, Aldrich-18225-7[41]) was also measured to be 1.11 ± 0.03.

For the dPS in toluene-*d*, ν has a value between 1.15 and

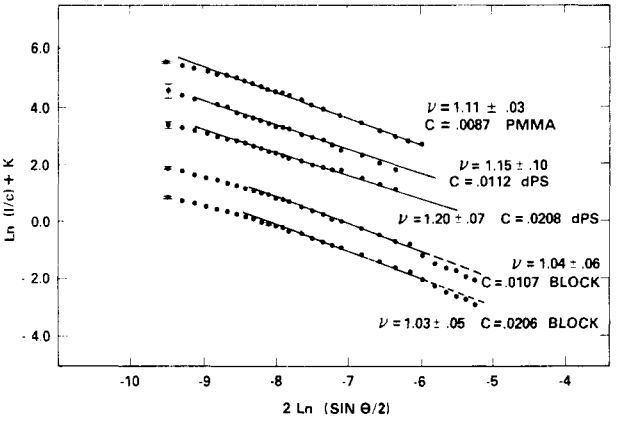

Figure 7. ln $(I/c) + K$ vs. 2 ln $(\sin \theta/2)$ plot from neutron scattering data at large x limit.

1.20. Because of the uncertainty in the data, the concentration dependence of ν should not be taken seriously.

In Table II, we have summarized all the results we have obtained. The PMMA block in the diblock copolymer has the molecular weight more than twice that of the dPS block. But it is very compact, with a near theta configuration and radius of gyration $\langle R_G^2 \rangle^{1/2}$ = 85 Å and ν = 1. This is surprising since toluene at 23 °C should be a good solvent for the PMMA as evidenced by ν = 1.11 for the Aldrich-18225-7 PMMA and the viscosity molecular weight data[34] of $[\eta] \propto M^{0.73}$. On the other hand, the dPS block has a dimension only slightly bigger than its precursor. In other words, the dPS block expanded slightly but the PMMA block contracted a great deal and its radius of gyration of 85 + 7 Å can be compared with that of 100 Å for the theta condition, calculated by using a characteristic ratio of 6.9 and a carbon–carbon bond length of 1.53 Å.[33,35]

A question that immediately arises is "what is the configuration of this dPS–PMMA diblock copolymer in toluene?" We suggest the following plausible models which should not exclude other more complicated possibilities: (1) completely unsegregated model; (2) completely segregated dumb-bell model; (3) completely segregated core and shell (micell) model; (4) partially segregated dumb-bell model; (5) partially segregated core and shell model. The first three are perhaps too primitive. We could eliminate them immediately for the following reasons: (1) For the completely unsegregated model, we would expect both blocks to have an expanded conformation. Since the PMMA block is contracted in a near-theta configuration, this model cannot represent the block copolymer in toluene. (2) For the second model, both blocks are expected to have about the same dimension as their respective homopolymers because of the absence of heterosegmental contacts. This is certainly not true for the PMMA block. (3) For the third model, we would expect the dPS block to have a bigger radius of gyration than that of its precursor. Since we found it to be only slightly expanded, we must conclude that

Table II
Summary of Experimental Results

	Mol wt	$\langle R_G^2 \rangle^{1/2}$, Å	Excluded vol exponent ν	2nd virial coefficient A_2, mol ml/g^2
dPS (homo)	(88 ± 3) × 10^3 (LS)	215 ± 18 (LS) 210 ± 40 (NS)	1.15–1.20 (NS)	(5.2 ± 1.0) × 10^{-4} (LS)
dPS (block)	[(95 ± 3) × 10^3 (LS)]	225 ± 40 (LS)		
PMMA (block)	203 × 10^3 (EA)	85 ± 7 (NS)	1.03 ± 0.05 (NS)	
PMMA (homo)	60.6 × 10^3		1.11 ± 0.03 (NS)	

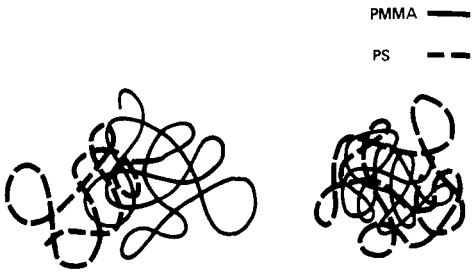

Figure 8. A representation of model (4) (left) and model (5) (right) of the dPS–PMMA block copolymer configuration.

the dPS block has a random coil segmental distribution function having radial symmetry and with higher segment density at the center of mass position.

After eliminating the above three models, we are left with the partially segregated models (4) and (5) depicted in Figure 8. Again, model (4) can be rejected by the argument that it ought to give an expanded dimension for both blocks caused by some heterosegmental repulsions.

We find therefore that model (5) is the only simple one which is consistent with our observations and appears to be reasonable in terms of our knowledge of diblock copolymers.

V. Conclusions

In this study we have utilized some unique features of SANS together with LS and we have found that the PMMA block in the diblock copolymer has a very different conformation compared to its homopolymer state. The near theta configuration of the PMMA block in conjunction with the slightly expanded dimension of the dPS block leads to a partially segregated core and shell model of the PS–PMMA diblock copolymer in toluene. In other words, the PMMA block is in a compact configuration and forms a central core and as a result of the repulsive interactions between the PS block and the PMMA block, the PS is somewhat pushed toward the outside. The fact that toluene is a better solvent for PS than for PMMA may be responsible for such a configuration.

With this configuration one would expect that neighboring polymer molecules will not be completely interpenetrable and the correlation function for the center of mass of polymer molecules may be governed by a "hard-sphere-like" (by no means of rigid hard sphere) interaction potential. In such a case the structure factor $S'(\mathbf{q})$ should be given by the one shown in the upper part of Figure 9. From eq 14, we know also that the total structure factor $I(\mathbf{q})$ is the product of the external part $S'(\mathbf{q})$ and the internal part $P(\mathbf{q})$ which should correspond to a random coil profile[20] as shown in the lower part of Figure 9. The product of these two will give a maximum at around the first peak of $S'(\mathbf{q})$ which occurs at a q^{-1} corresponding to the dimension of this inpenetrable hard sphere. Thus the maximum of $I(\mathbf{q})$ should represent the upward curvature or the "anomaly" in the Zimm plot since the Zimm plot is just an inverse plot of $I(\mathbf{q})$.

Two points must be noted here: (1) Whether one will be able to observe the upward curvature in the Zimm plot or not depends on the relative contribution from the internal vs. the external correlation in eq 14 and the $\mathbf{q}$ range where the scattering experiment is carried out. Normally, the upward curvature is observed in the case of large molecular weights[7,8] (with $M \gtrsim 10^6$) at $q \lesssim 0.005$ Å^{-1}. But, since the external part is weighted by the concentration as shown in eq 14, we would expect similar behavior in the Zimm plot from the external correlation effect for smaller polymer molecules at higher concentration; however, these concentrations are not in the range of concentration for our measurements. As we increase

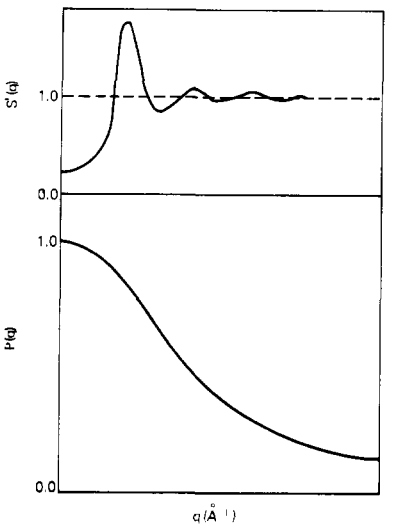

Figure 9. A representation for the structure factor of a hard sphere-like liquid $S'(q)$ and the particle scattering factor of a coillike polymer molecule $P(q)$.

concentration, we observed the onset of the multimolecular micell (at about 6%) structure occurring before the upward curvature begins to be seen in the Zimm plot of our light scattering experiment.

Furthermore, a positive concentration dependence of $c/\mathrm{I}(\mathbf{q})$ was observed in the light scattering experiment of this block copolymer, contrary to the neutron scattering data which have shown a zero concentration dependence. Although the light scattering was looking at the dPS block while the neutron scattering was looking at the PMMA block the external part of the structure factor $S'(\mathbf{q})$ should be governed by the same center of mass correlation. Therefore we would expect similar concentration dependence. At first, this seems to be contradictory. But we will have to remember that the smallest q in our neutron scattering experiment is 0.01 Å^{-1}. At this q, $\mathrm{S}'(\mathbf{q})$ probably has passed the initial peak and is reaching the asymptotic limit of 1. In other words $\int h(\mathbf{r})e^{-i\mathbf{q}\cdot\mathbf{r}}\,d\mathbf{r}$ has approached zero and gives the zero concentration dependence in the Zimm plot.

(2) The hard-sphere interaction potential approach has been proposed by Doty et al.[36,37] for descriptions of Bovine Serum Albumin and polymethacrylic acid, by Burchard[38] for poly(vinyl carbanilate), and by Bywater[9] and Utiyama[7] for block copolymers. In this paper, we have offered an explicit physical explanation as to why this external correlation approach is more applicable to the block copolymer case than the segmental contact approach developed by Zimm[39] and Albrecht[40] which was aimed mainly at random coil homopolymers. One should be able to obtain better estimates of the dimension and the molecular weight of the block copolymer from light scattering experiments by including the external part of the structure factor caused by the partially segregated core and shell conformation.

Acknowledgment. The authors wish to thank Dr. D. H. Reneker for his support and Professor H. Yu for the preparation of the polymer sample. We also acknowledge Dr. J. Mazur and Dr. F. L. McCrackin for their helpful discussion and collimation correction.

References and Notes

(1) D. C. Allport and W. H. Janes, Ed., "Block Copolymers", Wiley, New York, N.Y., 1973.
(2) G. M. Burnett, P. Meares, and C. Paton, *Trans. Faraday Soc.*, **58**, 737 (1962).
(3) A. Dondos, D. Froelich, P. Rempp, and H. Benoit, *J. Chim. Phys. Phys.-Chim. Biol.*, **64**, 1012 (1967).

(4) A. Dondos, P. Rempp, and H. Benoit, *Polymer*, **16**, 698 (1975).
(5) S. Krause, *J. Phys. Chem.*, **68**, 1948 (1964).
(6) H. Utiyama, K. Takenaka, M. Mizumori, M. Fukuda, Y. Tsunashima, and M. Kurata, *Macromolecules*, **7**, 515 (1974).
(7) H. Utiyama, K. Takenaka, M. Mizumori, and M. Fukuda, *Macromolecules*, **7**, 28 (1974).
(8) T. Tanaka, T. Kotaka, and H. Inagaki, *Macromolecules*, **7**, 311 (1974).
(9) J. Prud'homme and S. Bywater, *Macromolecules*, **4**, 543 (1971).
(10) J. G. Zilliox, J. E. L. Roovers, and S. Bywater, *Macromolecules*, **8**, 573 (1975).
(11) J. P. Cotton, D. Decker, H. Benoit, B. Farnoux, J. Higgins, J. Jannink, R. Ober, C. Picot, and J. des Cloizeaux, *Macromolecules*, **7**, 863 (1974).
(12) R. G. Kirste, W. A. Kruse, and J. Shelten, *J. Makromol. Chem.*, **162**, 299 (1972).
(13) D. G. H. Ballard, J. Shelten, and C. D. Wignall, *Eur. Polym. J.*, **9**, 965 (1973).
(14) J. P. Cotton, D. Decker, B. Farnoux, G. Jannink, R. Ober, and C. Picot, *Phys. Rev. Lett.*, **32**, 1170 (1974).
(15) R. G. Kirste and W. A. Kruse, *Polymer*, **16**, 120 (1975).
(16) J. P. Cotton, B. Farnoux, and G. Jannink, *J. Chem. Phys.*, **57**, 290 (1972).
(17) J. S. King, G. C. Summerfield, and R. Ullman, *Polym. Prepr., Am. Chem. Soc., Div. Polym. Chem.*, **16**, 410 (1975).
(18) For example: F. Kohler, "The Liquid State", Verlag Chemie, Weinheim/Bergstr., Germany, 1972; Chapter 4, or H. Boutin and S. Yip, "Molecular Spectroscopy with Neutrons", MIT Press, Cambridge, Mass., 1968.
(19) A. S. Hyman, *Macromolecules*, **8**, 849 (1975).
(20) For example: M. B. Huglin, Ed., "Light Scattering from Polymer Solutions", Academic Press, New York, N.Y., 1972; or H. Yamakawa, "Modern Theory of Polymer Solutions", Harper and Row, New York, N.Y., 1971.
(21) F. Zernicke and J. A. Prins, *Z. Phys.*, **41**, 184 (1927).
(22) P. Debye and H. Menke, *Phys. Z.*, 797 (1930).
(23) For example: C. Tanford, "Physical Chemistry of Macromolecules", Wiley, New York, N.Y., 1961.
(24) A. Peterlin, *J. Chem. Phys.*, **23**, 2464 (1955).
(25) A. J. Hyde, *Trans. Faraday Soc.*, **56**, 591 (1960).
(26) O. B. Ptitsyn, *Zh. Fiz. Khim.*, **31**, 1091 (1957); or ref 20, Chapter 7.
(27) J. Mazur and D. McIntyre, *Macromolecules*, **8**, 464 (1975).
(28) D. J. Coumou, *J. Colloid Sci.*, 408 (1960).
(29) J. H. O'Mara and D. McIntyre, *J. Phys. Chem.*, **63**, 1435 (1959).
(30) L. J. Fetters, *J. Res. Natl. Bur. Stand., Sect. A*, **70a**, 5, 421 (1966).
(31) G. E. Bacon, "Neutron Differaction", Oxford, 1962.
(32) J. Mazur, *Natl. Bur. Stand. (U.S.), Tech. Note*, in press.
(33) D. Y. Yoon and P. J. Flory, *Polymer*, **9**, 645 (1975).
(34) J. D. Matlack, A. L. Resnick, and R. J. Samuels, *J. Polym. Sci.*, **17**, 391 (1955).
(35) P. J. Flory, "Statistic Mechanics of Chain Molecules", Interscience, New York, N.Y., 1969.
(36) P. Doty and R. F. Steiner, *J. Chem. Phys.*, **20**, 85 (1952).
(37) A. Oth and P. Doty, *J.* Phys. Chem., **56**, 43 (1952).
(38) W. Burchard, *Polymer*, **10**, 29 (1969).
(39) B. H. Zimm, *J. Chem. Phys.*, **16**, 1093 (1948).
(40) A. C. Albrecht, *J. Chem. Phys.*, **27**, 1014 (1957).
(41) Certain commercial materials and equipment are identified in this paper in order to specify adequately the experimental procedure. In no case does such identification imply recommendation or endorsement by the National Bureau of Standards, nor does it imply that the material or equipment identified is necessarily the best available for this purpose.

Conformation of Flexible Polymers Near an Impermeable Surface

Takeshi Tanaka

Laboratory of Polymer Separation and Characterization, Institute for Chemical Research, Kyoto University, Uji, Kyoto, 611, Japan. *Received April 15, 1976*

ABSTRACT: Statistics on a random-flight chain which is bound on or near an impermeable, noninteracting planar surface with one end or both ends were developed. Probability densities of finding a given number of segments at respectively specified locations were obtained as functions of the location(s) of end segment(s). From these functions some new information about the conformational properties of flexible polymers near the surface was derived such as overall density distribution of segments and moments of segment distribution about the end segment and about the center of mass, all as functions of the location(s) of end segment(s). As for the so-called "tail" chain, the first-order coefficient of the perturbation theory of excluded-volume effects concerning the mean-square end-to-end distance was also derived.

The statistics of random flights near impermeable surfaces are important in understanding the behavior of flexible polymer molecules under various situations such as adsorption onto interfaces, stabilization of colloidal dispersions, partition equilibrium in gel permeation chromatography, and two-phase formation in crystalline polymers and in block copolymers. In particular, random-flight chains attached on a flat surface with one end ("tail" chain) or both ends ("loop" chain) are important as the simplest models. For these models the probability densities $f_n(Z_i)$ of finding the ith segment of a chain with size n at a normal-to-surface distance Z_i have been obtained by Hoeve,[1] Meier,[2] and Hesselink,[3] and the overall density distribution of segments has been calculated.[3] Recently, Lax[4] examined the effects of volume exclusion between segments on the function $f_n(Z_i)$ by a method of exactly enumerating the number of self-avoiding walks on a lattice.

In this paper we also deal with a random-flight chain near a planar surface. We first formulate the conditional probability densities $P_n(Z_i, Z_j, Z_k, \ldots)$ of finding series of segments $(i, j, k, \ldots)$ at respective positions $(Z_i, Z_j, Z_k, \ldots)$, when the chain is bound at given distance(s) from the surface with one end ("taillike" chain) or both ends ("looplike" chain). This generalization enables us to calculate various quantities of interest such as overall density distribution of segments as a function of the distance(s) of the end segment(s) from the surface, moments of segment distribution about the end segment and about the center of mass, and coefficients of perturbation theory of excluded-volume effects. The moments are important especially when we deal with radiation scattering from such molecules. The perturbation theory offers another approach to the excluded-volume problem. Some results on these points will be given below.

Formulation

Consider a random-flight chain with $n + 1$ segments (size n) serially numbered from 0 to n. Assuming an impermeable, noninteracting plane at $Z = 0$ of orthogonal coordinate system (X, Y, Z), we can write the conditional probability density $P_n(Z_n/Z_0)$ of finding the last (nth) segment at Z_n with the first (0th) segment fixed at $Z_0 \geq 0$, as[5,2]

$$P_n(Z_n/Z_0) = K_1 \{\exp[-\beta_{0n}(Z_0 - Z_n)^2] - \exp[-\beta_{0n}(Z_0 + Z_n)^2]\} \quad (1)$$

Here K_1 is the normalization constant given by

$$K_1 = (\beta_{0n}/\pi)^{1/2}/\mathrm{erf}(\beta_{0n}{}^{1/2}Z_0) \quad (2)$$